Defence Science Journal, Vol. 74, No. 3, May 2024, pp. 360-364, DOI : 10.14429/dsj.74.19900

Effect of Porosity on the Free Vibration Analysis of a Rotating Pretwisted Sandwich Blade with a Functionally Graded Core in the Thermal Environment

Shashank Pandey

Mechanical Engineering Department, National Institute of Technology, Jamshedpur - 831 014, India
E-mail: shashankpandey200@gmail.com

ABSTRACT

This work deals with the investigation of the effect of porosity on the natural frequencies of the rotating pre twisted sandwich blade with a functionally graded core in the thermal environment. The top metallic and the bottom ceramic surfaces are exposed to ambient temperature and high inlet temperature, respectively. A finite element approach using a layer wise theory is developed. Two different porosity distributions are assumed here. The effect of the volume fraction index, rotational velocity, porosity model and temperature gradient on the natural frequencies of the pre twisted sandwich blade is studied.

Keywords: Free vibration analysis; Porosity; FEM; Thermal environment; Rotating pre twisted FGM sandwich blade; Layer wise theory

1. INTRODUCTION

Turbine blades are mostly exposed to high-temperature environments (Ansari[1], *et al.*). The combined effect of the higher rotational velocity and the temperature requires careful design and analysis. It is well known that blades made of advanced materials like functionally graded material (FGM) have an advantage in terms of long service life and better operational efficiency[2]. Interestingly, during the process of manufacturing, voids are created in the layers made of functionally graded material (FGM)[3]. Researchers like Chen[2], *et al.* investigated the natural frequencies of the rotating pre twisted functionally graded material (FGM) blade in a thermal atmosphere. Yan[4], *et al*. investigated the nonlinear transient response of the rotating blade made of FGM using a new structure dynamic model. Singha[5], *et al.* studied the behaviour of the natural frequency of the pre twisted rotating panel. Chen[6], *et al.* presented a rotational dynamic model based on a quasi-three-dimensional approach for rotating pre-twisted FGM blades. The application of the finite element method (FEM) has several benefits. Researchers like Singha[7], *et al.*, Parida and Mohanty[8], Karmakar and Sinha[9], Karakoti[10], *et al.* used FEM to perform dynamic analysis of the FGM pre twisted rotating blade and FGM panels.

The exhaustive review of the literature indicates that there is limited work available on the investigation of natural frequencies of the rotating pre twisted blade with an FGM core in a thermal atmosphere employing a FEM formulation. Therefore, the present work aims to explore the output of the implementation of different porosity models on the fundamental vibrational modes of the rotating pre twisted sandwich blade with an FGM core in the thermal atmosphere. Ceramic and metal are used as the lower layer and the upper layer of the sandwich blade and the core is composed of FGM. The top metallic and the bottom ceramic surfaces are exposed to ambient temperature and high inlet temperature, respectively. A finite element method (FEM) formulation using a layer-wise approach is presented. Two different porosity distributions are taken up for this study. The principle based on Hamilton's approach is implemented to obtain the differential equation. Different parameters are varied to research the effect of distributions of porosity, gradient index, rotational velocities and temperature gradient on the natural frequencies of the blade.

2. MATHEMATICAL FORMULATION

Assume a sandwich blade with the upper, middle and lower surfaces composed of metal, porous FGM and ceramic. The FGM sandwich blade lies on a rectangular planform having width a and length b along the x and y axes as shown in Fig. 1. h is the thickness of the blade. h_1, h_2 and h_3 are the thicknesses of the upper, middle and lower surfaces. The upper, middle and lower layers of the FGM sandwich blade are made of pure metal, FGM and pure ceramic respectively. Ψ is the angle of the twist. It may be noted here that in the present analysis, a full three-dimensional problem is reduced to a two-dimensional analysis by assuming the thickness of the FGM sandwich blade small (Kashtalyan[11], *et al.*). The layer-wise theory is used as a displacement field for the present investigation and the same for the middle, the top and the bottom surface is given as[12]:

$$
\begin{aligned}
u^{(2)}(x,y,z) &= u_o(x,y) + z^{(2)}\theta_x^{(2)} \\
v^{(2)}(x,y,z) &= v_o(x,y) + z^{(2)}\theta_y^{(2)} \\
w^{(2)}(x,y,z) &= w_o(x,y)
\end{aligned}
\tag{1a}
$$

Received : 12 February 2024, Revised : 24 February 2024
Accepted : 04 March 2024, Online published : 10 May 2024

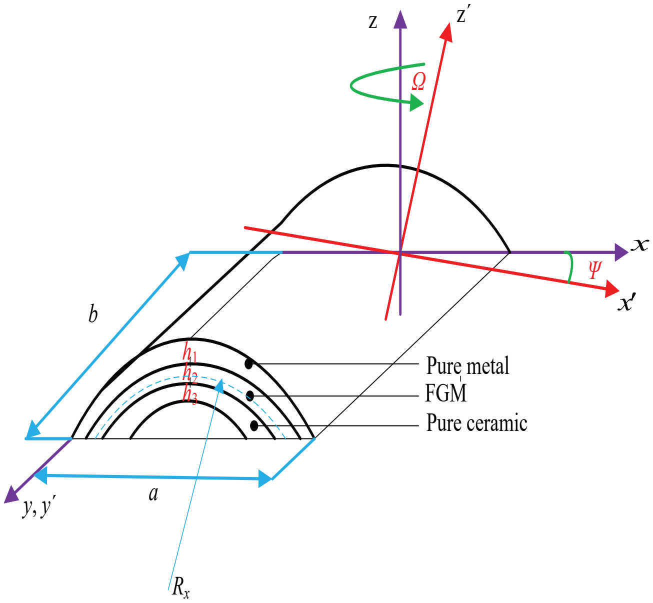

Figure 1. Pre-twisted rotating sandwich blade with FGM core.

$$
\begin{aligned}
u^{(3)}(x,y,z) &= u_0(x,y) + z^{(3)}\theta_x^{(3)} + (h_2/2)\theta_x^{(2)} + (h_3/2)\theta_x^{(3)} \\
v^{(3)}(x,y,z) &= v_0(x,y) + z^{(3)}\theta_y^{(3)} + (h_2/2)\theta_y^{(2)} + (h_3/2)\theta_y^{(3)} \\
w^{(3)}(x,y,z) &= w_0(x,y)
\end{aligned}
\tag{1b}
$$

$$
\begin{aligned}
u^{(1)}(x,y,z) &= u_0(x,y) + z^{(1)}\theta_x^{(1)} + (h_2/2)\theta_x^{(2)} + (h_1/2)\theta_x^{(1)} \\
v^{(1)}(x,y,z) &= v_0(x,y) + z^{(1)}\theta_y^{(1)} + (h_2/2)\theta_y^{(2)} + (h_3/2)\theta_y^{(1)} \\
w^{(1)}(x,y,z) &= w_0(x,y)
\end{aligned}
\tag{1c}
$$

The displacement at a coordinate in *the* x, y and z system is given by $u^{(i)}$, $v^{(i)}$ and $w^{(i)}$ for any i^{th} layer (i = 1, 2 and 3). The transverse displacement is given as w_o and the same is constant for all the three layers. u_o and v_o are the in plane displacements in x and y directions at the middle plane. The small inclination of normal having rotation to mid-plane with y and x-axes is given by $\theta_x^{(i)}$ and $\theta_y^{(i)}$. Accordingly, the strain-displacement relationship is given as[7,13]:

$$
\begin{aligned}
\varepsilon_{xx}^{(i)} &= \frac{\partial u^{(i)}}{\partial x} = \varepsilon_x^0 + z^{(i)}\kappa_{xx}^{(i)} \\
\varepsilon_{yy}^{(i)} &= \frac{\partial v^{(i)}}{\partial y} = \varepsilon_y^0 + z^{(i)}\kappa_{yy}^{(i)} \\
\gamma_{xy}^{(i)} &= \frac{\partial u^{(i)}}{\partial y} + \frac{\partial v^{(i)}}{\partial x} + \frac{2w^{(i)}}{R_{xy}} = \gamma_{xy}^0 + z^{(i)}\kappa_{xy}^{(i)} + \frac{2w^{(i)}}{R_{xy}}
\end{aligned}
\tag{2}
$$

$$
\varphi_x^{(i)} = \theta_x^{(i)} + \frac{\partial w^{(i)}}{\partial x},\ \varphi_y^{(i)} = \theta_y^{(i)} + \frac{\partial w^{(i)}}{\partial y},
$$

$$
\varepsilon_x^0 = \frac{\partial u_0}{\partial x} + \frac{w}{R_x},\ \kappa_{xx}^{(i)} = \frac{\partial \theta_x^{(i)}}{\partial x},\ \kappa_{yy}^{(i)} = \frac{\partial \theta_y^{(i)}}{\partial y},\ \kappa_{xy}^{(i)} = \frac{\partial \theta_y^{(i)}}{\partial x} + \frac{\partial \theta_x^{(i)}}{\partial y}
$$

are plate curvatures. The middle plane of the curved blade is given as $z^{(i)} = -\dfrac{x^{(i)}y^{(i)}}{R_{xy}}$ where, $R_{xy} = \dfrac{a}{\tan\psi}$. ε_x^0 and ε_y^0 are the in plane strains in x and y directions at the midplane and γ_{xy}^0 is the in plane shear strain at the midplane. $\kappa_{xx} = \partial\theta_x/\partial x$ and $\kappa_{yy} = \partial\theta_y/\partial y$ are the derivatives of the rotational. $\varphi_x^{(i)}$ and $\varphi_y^{(i)}$ are the shear strain components of any i^{th} layer. R_x is the radius of curvature in the x-direction. R_{xy} is the pre-twist radius. Since the upper and lower layers are made of isotropic materials a constant temperature is assumed for the same. However, the middle layer is made of FGM having gradation along the thickness direction and the solution for the temperature profile is obtained from the Fourier law of heat conduction equation under steady state (Eqn. 3) that results in a nonlinear profile of temperature along the thickness (Karakoti[10]*, et al.*):

$$
-\frac{d}{dz}\left[K^{(i)}(z,T)\frac{dT^{(i)}}{dz}\right] = 0 \tag{3}
$$

The temperature field ($T^{(i)}$) and the thermal conductivity ($K^{(i)}$) have nonlinear variation across the thickness[14].

2.1. Porous FGM With Even Porosity

In this estimation, the temperature-dependent elastic property at any point ($P^{(i)}$) along the thickness (z) direction is given by[15]:

$$
P^{(i)}(z,T) = [P_m(T) - P_c(T)]\lambda^{(i)} + P_c(T) - \frac{\xi}{2}[P_m(T) + P_c(T)] \tag{4}
$$

where, $P_c(T)$ and $P_m(T)$ are elastic properties of ceramic and metal respectively and the same depends on the temperature. ξ is the porosity coefficient. $\lambda^{(i)}$ is the volume fraction of pure metal constituent for any i^{th} layer and the same is expressed as:

$$
\lambda^{(i)} = \left(2z^{(i)} + h\right)^n \Big/ 2h \tag{5}
$$

n is a non-negative real number that determines the volume fraction profile of metal in functionally graded core across their thickness.

2.2 Porous FGM With Uneven Porosity

In the uneven distribution of porosity, the temperature-dependent elastic property is given as[15]:

$$
\begin{aligned}
P^{(i)}(z,T) &= [P_m(T) - P_c(T)]\lambda^{(i)} + \\
&P_c(T) - \frac{\xi}{2}[P_m(T) + P_c(T)]\left[1 - \frac{z - h_2}{h_1 - h_2}\right]
\end{aligned}
\tag{6}
$$

Eqns. (4-6) are used to obtain the material property at a point along the thickness direction for the upper metallic, the middle FGM and the lower ceramic layer of the sandwich blade having FGM core. The obtained material properties are used in the derivation of the rigidity matrix (D) and the inertia matrix (I) that are further used in the derivation of the global stiffness matrix (K), global geometric thermal stiffness matrix (KσTH), global geometric rotational stiffness matrix (KσR) and mass matrix (M) in the FEM formulation. Further, Lagrange's equation of motion is used to obtain the governing differential equation and the first variation of the linear strain energy, kinetic energy, thermal and rotational load-based strain energy are taken. The global stiffness matrix (K), mass matrix (M) are derived using linear strain energy and kinetic energy[16]. However, the geometric stiffness matrix ($K_{\sigma TH}$) due to thermal load is derived from the non-linear strain energy ($U_{nl\text{-}TH}$) as:

$$
\mathbf{U_{nl\text{-}TH}} = \int_V \boldsymbol{\sigma}_t^T \boldsymbol{\varepsilon}_{\mathbf{nl}}\, dV \tag{7}
$$

where, σ_t and ε_{nl} is the initial stress vector and non-linear strain vector, respectively. Further, the non-linear strain ($U_{nl\text{-}TH}$) is expressed in terms of initial stress and differential matrix (g) for any j^{th} element as:

$$\mathbf{U}_{\mathbf{nl\text{-}TH}\,j} = \frac{1}{2}\int_A \mathbf{g}_j^T \mathbf{S}_{\boldsymbol{\sigma}\mathbf{TH}\,j}\mathbf{g}_j \, dA \tag{8}$$

also, $g_j = G_j d_j$ (9)

Where,

$$\mathbf{d}_j = \left\{u_0,\ v_0,\ w_0,\ \theta_x^{(1)},\ \theta_y^{(1)},\ \theta_x^{(2)},\ \theta_y^{(2)},\ \theta_x^{(3)},\ \theta_y^{(3)}\right\}_j$$

is the nodal displacement vector for any j^{th} layer. G_j and $S_{\sigma j}$ are the, differential matrix and initial stress matrix due to the thermal load of any j^{th} element. Substituting Eq. (9) in Eq. (8). The total strain energy due to thermal load and non-linear strain is given as:

$$\mathbf{U}_{\mathbf{nl\text{-}TH}} = \sum_{j=1}^{N}\frac{1}{2}\int_A \mathbf{g}_j^T \mathbf{S}_{\sigma\mathrm{TH}\,j}\mathbf{g}_j \, dA \tag{10}$$

$$\mathbf{U}_{\mathbf{nl\text{-}TH}} = \sum_{j=1}^{N}\frac{1}{2}\int_A \mathbf{d}_j^T \mathbf{k}_{\sigma\mathrm{TH}\,j}\mathbf{d}_j \tag{11}$$

Where, $k_{\sigma j}$ is the geometric stiffness matrix due to the thermal load of any j^{th} element and the same is expressed as:

$$\mathbf{k}_{\sigma\mathrm{TH}\,j} = \int_A \mathbf{G}_j^T \mathbf{S}_{\sigma\mathrm{TH}\,j}\mathbf{G}_j \tag{12}$$

At the elemental level ($k_{\sigma THj}$) is assembled to get the global thermal geometric stiffness matrix ($k_{\sigma TH}$) for the entire porous FGM sandwich blade. Similarly, the geometric stiffness matrix due to rotation ($k_{\sigma R}$) is derived.

Lagrange's equation of motion is used to obtain the governing differential equation as:

$$\mathbf{M}\ddot{\mathbf{d}} + \left(\mathbf{K} + \mathbf{K}_{\boldsymbol{\sigma}\mathbf{TH}} + \mathbf{K}_{\boldsymbol{\sigma}\mathbf{R}}\right)\mathbf{d} = 0 \tag{13}$$

Now, the separation of time and space is done to obtain the generalized Eigen value problem. Further subspace iteration method is used to obtain the natural frequency for the present analysis[17].

3. RESULTS AND DISCUSSION

The natural frequencies of a single-layered FGM plate are discussed here. The bottom and the top layer of the FGM plate are composed of aluminum (Al, ρ_m = 2703 Kg/m^3, v_m =0.3, E_m = 70 GPa,) and aluminum oxide (Al_2O_3, ρ_c = 3800 Kg/m^3, v_c =0.3, E_c = 380 GPa,), respectively. Table 1 presents the natural frequencies for an FGM plate which is simply supported, for an *a*/*h* ratio of 20, taking the porosity coefficient (ξ) as 0.4 and gradient index (n) is taken as 1. As evident from Table 1 that the present FEM formulation gives results that have an error of 1.098% and 1.321% with respect to the analytical solution given by Demirhan and Taskin[18]. It is also found that a mesh of 6 × 6 gives accurate results. Thus, it can be inferred that the present FEM formulation is accurate, computationally efficient and simple.

Table 1. Natural frequencies of a single-layered FGM plate (*a*/*h* = 20, ξ = 0.4, *n* = 1)

	Even	Uneven
Demirhan & Taskin[18]	0.0182	0.0227
Present	0.0184	0.0230

Further, the influence of gradient index (n) on the non-dimensional natural frequencies ($\varpi = \omega(a^2/h)\sqrt{\rho_m(1-v_m^2)/E_m}$)[16] of pretwisted sandwich blade with porous FGM core having 1-8-1 configuration is presented. The elastic properties of Zirconia-Oxide (ZrO_2) and Titanium alloy (Ti-6Al-4V) that depend on the temperature are taken for the present analysis[19]. Fig. 2 presents the variation of ϖ with n for different porosity models.

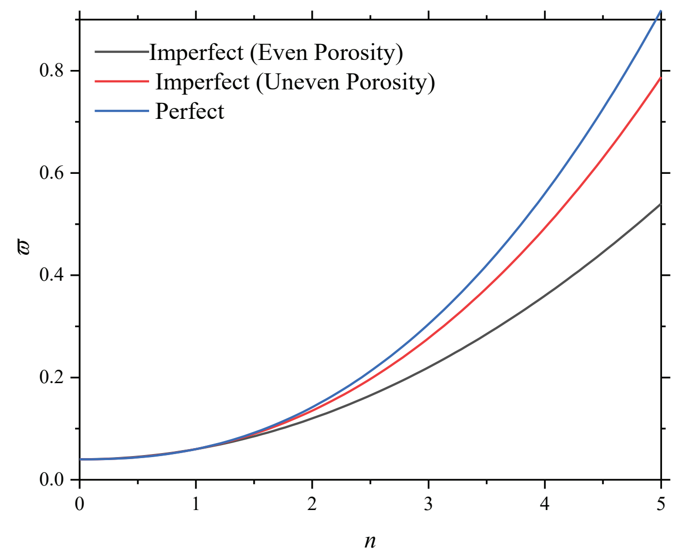

Figure 2. Variation of ϖ of a 1-8-1 pre-twisted sandwich blade with homogenous facesheets and FGM core for different porosity models (a/h = 20, ξ = 0.2, Ψ = 30°, ΔT = 300 K).

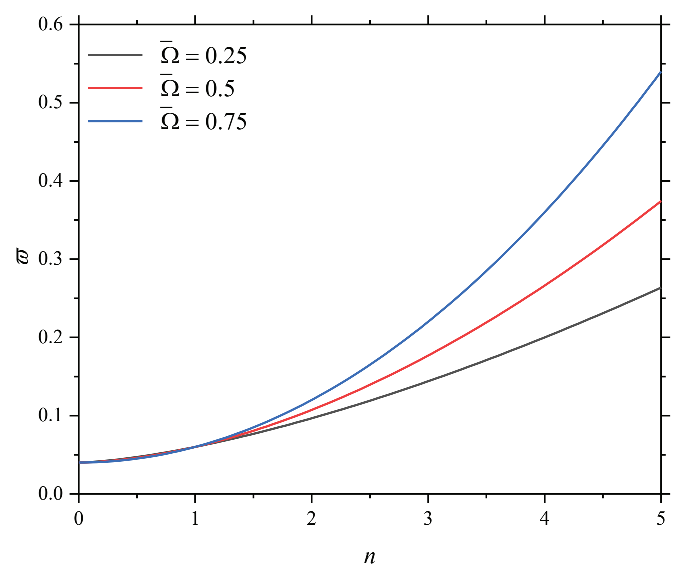

Figure 3. Variation of ϖ of a 1-8-1 imperfect-even porosity pre-twisted sandwich blade with homogenous facesheet and FGM core for various non-dimensional rotational velocities ($\bar{\Omega}$) (a/h = 20, ξ = 0.2, Ψ = 30°, ΔT = 300 K).

It is observed from Fig. 2 that the variation of ϖ for a 1-8-1 rotating blade with homogenous face sheets and FGM core, increases monotonically for the n varying from 0 to 5, taking non-dimensional rotational velocity ($\overline{\Omega} = \Omega/\omega_0$) and pre-twist angle ($\Psi$) as 0.75 and 30°, respectively. It may be noted here that the present results are obtained using a 6 × 6 mesh. The same is observed maximum for a sandwich blade with no porosity (perfect blade) followed by an FGM sandwich blade with imperfect porosity having uneven distribution of the same. However, $\overline{\omega}$ is observed to be minimum for the FGM sandwich blade with imperfect porosity having even distribution.

Next, the effect of varying the non-dimensional rotational velocity ($\overline{\Omega} = \Omega/\omega_0$) on ϖ of the imperfect sandwich panel having an even distribution of porosity is investigated. Figure 3 presents the variation of ϖ of a 1-8-1 imperfect even-porosity prewisted sandwich blade for non-dimensional rotational ($\overline{\Omega}$) velocities of 0.25, 0.5 and 0.75. It is found from Fig. 3 that ϖ increases with an increase in $\overline{\Omega}$ from 0.25 to 0.5 and the same is observed maximum for $\overline{\Omega}$ = 0.75. It may also be noted here that with the increase in the porosity, the stiffness of the FGM panel decreases and the natural frequency decreases[15].

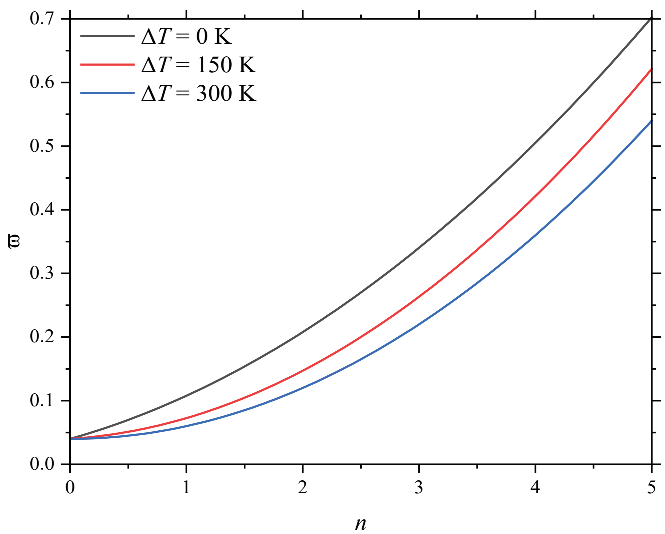

Figure 4. Variation of $\overline{u}$ of a 1-8-1 imperfect-even porosity pre-twisted sandwich blade with homogenous facesheet and FGM core for various temperature gradients (a/h = 20, ξ = 0.2, ϕ = 30°, $\overline{\Omega} = 0.75$).

Next, the effect of varying the temperature gradient ΔT on ϖ of the imperfect sandwich panel having an even distribution of porosity is investigated. Figure 4 presents the variation of ϖ of a 1-8-1 imperfect even-porosity prewisted sandwich blade for temperature gradient of ΔT = 300K, 150K and 0K. It is observed from Fig. 4 that ϖ increases with the decrease in ΔT from 300 to 0 and the same is observed maximum for non-thermal loading viz. ΔT = 0 K.

4. CONCLUSIONS

This study deals with the free vibration study of the FGM sandwich blade. Several parameters are explored to observe the effect of gradient index, porosity model, rotational velocity and temperature gradient on natural frequencies of the pretwisted sandwich blade having a core made of FGM considering the thermal conditions. The concluding remarks of this investigation are discussed as follows:

- The natural frequency is highest for the gradient index of 5
- With the increase in the rotational velocity, the natural frequency increases
- With the rise in the gradient index, the fundamental frequency increases
- The present finite element formulation is general, simple and accurate for the analysis of rotating FGM panels
- The results present in this work for the free vibration analysis of porous FGM rotating blade will serve as a benchmark problem.

REFERENCES

1. Ansari, E.; Setoodeh, A.R. & Rabczuk, T. Isogeometric-stepwise vibrational behavior of rotating functionally graded blades with variable thickness at an arbitrary stagger angle subjected to thermal environment. *Compos. Struct*., 2020, **244,** 112281.
doi: 10.1016/j.compstruct.2020.112281
2. Chen, Y.; Ye, T; Jin, G; Li, S. & Yang, C. Vibration analysis of rotating pretwist FG sandwich blade operating in thermal environment. *Int. J. Mech. Sci.,* 2021, 106596.
doi: 10.1016/j.ijmecsci.2021.106596
3. Wattanasakulpong, N. & Ungbhakorn V. Linear and nonlinear vibration analysis of elastically restrained end FGM beams with porosities. *Aero. Sci. Tech.*, 2014, **32**,111-120.
doi: 10.1016/j.ast.2013.12.002
4. Yan, N.; MingHui, Y. & Wei, Z. Nonlinear transient responses of rotating twisted FGM cylindrical panels. *Sci. Chi. Tech. Sci*., 2019, **62**, 317-330.
doi: 1.0. 10.0.7./.s1.1.4.3.1-.0.1.9.-1.4.7.2-1
5. Singha, T.D.; Rout, M., Bandyopadhyay, T. & Karmakar A. Free vibration of rotating pretwisted FG-GRC sandwich conical shells in thermal environment using HSDT. *Compos. Struct.*, 2021, **257**, 113144.
doi: 10.1016/j.compstruct.2020.113144
6. Chen, Y; Jin, G; Ye, T. & Chen, M. A quasi 3D dynamic model for free vibration analysis of rotating pre-twisted functionally graded blades. *J. Sound Vib.*, 2021, **499**, 115990.
doi: 10.1016/j.jsv.2021.115990
7. Singha, T.D.; Bandyopadhay, T. & Karmakar, A. Thermoelastic free vibration of rotating pretwisted sandwich conical shell panels with functionally graded carbon nanotube-reinforced composite facesheet using higher-order shear deformation theory. *Pro. Inst. Mech. Engg. Part L: J. Mat: Des. App.,* 2021, **235**(10), 2227-2253.
doi: 10.1177/1464420721999412
8. Parida, S.C. & Mohanty, S.C. Free vibration analysis of rotating functionally graded material plate under nonlinear thermal environment using higher order shear deformation theory. *J. Mech. Eng. Sci.*, 2018, 1-18.
doi: 10.1177/0954406218777535
9. Karmakar, A. & Sinha, P.K. Finite element free vibration analysis of rotating laminated composite pretwisted cantilever plates. *J. Rein. Plas. Comp.*, 1997, 1461-1491.
doi: 10.1177/07316844970160160

10. Karakoti, A.; Pandey, S. & Kar, V.R. Nonlinear transient analysis of porous P-FGM and S-FGM sandwich plates and shell panels under blast loading and thermal environment. *Thin Wall. Struct.*, 2022, **173**, 108985. doi: 10.1016/j.tws.2022.108985
11. Kashtalyan, M.; Kienzler, R. & Coors, M.M. Development of the consistent second-order plate theory for transversely isotropic plates and its analytical assessment from the three-dimensional perspective. *Thin Wal. Struct*., 2021, **163**, 107704. doi:10.1016/j.tws.2021.107704.
12. Ferreira, A.J.M. Analysis of composite plates using a layerwise theory and multiquardrics discretization. *Mech. Adv. Mat. Struct.*, 2005, **12**(2), 99-112. doi: .1016/j.compstruct.2015.07.101
13. Parhi, P.K.; Bhattacharyya, S.K. & Sinha P.K. Dynamic analysis of multiple delaminated composite twisted plate. *Air. Engg. Aero. Tech.*, 1999, **71**(5), 451-461. doi: 10.1108/00022669910296891
14. Javaheri, R. & Eslami, M.R. Thermal buckling of functionally graded plates based on higher-order theory. *J. Ther Stress.*, 2011, **25**(7), 603-625. doi: 10.1080/01495730290074333
15. Daikh, A.A. & Zenkour, A.M. Free vibration and buckling of porous power-law and sigmoid functionally graded sandwich plates using a simple higher-order shear deformation theory. *Mat. Res. Exp.*, 2019, **6**(11), 115707. doi: 10.1088/2053-1591/ab48a9
16. Pandey, S.; Pradyumna, S. Free vibration of functionally graded sandwich plates in thermal environment using a layerwise theory, *Eur. J. Mech. A/Solids*, 2015, **51**, 55-66. doi:10.1016/j.euromechsol.2014.12.001
17. Pradyumna, S. & Bandyopadhyay, J.N. Free vibration analysis of functionally graded curved panels using a higher-order finite element formulation, *J. Sou. Vib.*, 2008, **318**, 176–192. doi: 10.1016/j.jsv.2008.03.056
18. Demirhan, P.A. & Taskin, V. Bending and free vibration analysis of Levy-type porous functionally graded plate using state space approach. *Compos. Part B*, 2019, **160**, 661-676. doi: 10.1016/j.compositesb.2018.12.020
19. Reddy, J.N. & Chin, C.D. Thermomechanical analysis of functionally graded cylinder and plate. *J. Ther. Stresses*, 1998, **21**(6), 593-626. doi: 10.1080/01495739808956165

CONTRIBUTOR

Dr Shashank Pandey obtained his PhD degree from IIT Delhi. He is currently working as an Assistant Professor in the department of Mechanical Engineering, National Institute of Technology Jamshedpur. His research interests are in Solid mechanics.